Communication

# Controlling the magnetic anisotropy of van der Waals ferromagnet Fe3GeTe2 through hole doping

Se Young Park, Dong Seob Kim, Yu Liu, Jinwoong Hwang, Younghak Kim, Wondong Kim, Jae-Young Kim, Cedomir Petrovic, Choongyu Hwang, Sung-Kwan Mo, Hyung-jun Kim, Byoung-Chul Min, Hyun Cheol Koo, Joonyeon Chang, Chaun Jang, Jun Woo Choi, and Hyejin Ryu

*Nano Lett.*, **Just Accepted Manuscript** • DOI: 10.1021/acs.nanolett.9b03316 • Publication Date (Web): 22 Nov 2019

# Controlling the magnetic anisotropy of van der Waals ferromagnet $Fe_3GeTe_2$ through hole doping

Se Young Park[1,2,†], Dong Seob Kim[3,†], Yu Liu[4], Jinwoong Hwang[5,6], Younghak Kim[7], Wondong Kim[8], Jae-Young Kim[9], Cedomir Petrovic[4], Choongyu Hwang[6], Sung-Kwan Mo[5], Hyung-jun Kim[3], Byoung-Chul Min[3], Hyun Cheol Koo[3], Joonyeon Chang[3], Chaun Jang[3,*], Jun Woo Choi[3,*], and Hyejin Ryu[3,*]

[1]*Center for Correlated Electron Systems, Institute for Basic Science (IBS), Seoul 08826, Korea*

[2]*Department of Physics and Astronomy, Seoul National University (SNU), Seoul 08826, Korea*

[3]*Center for Spintronics, Korea Institute of Science and Technology (KIST), Seoul 02792, Korea*

[4]*Condensed Matter Physics and Materials Science Department, Brookhaven National Laboratory, Upton, New York 11973, United States*

[5]*Advanced Light Source, Lawrence Berkeley National Laboratory, Berkeley, CA 94720, USA*

[6]*Department of Physics, Pusan National University, Busan 46241, Korea*

[7]*Pohang Accelerator Laboratory, Pohang University of Science and Technology, Pohang 37673 Korea*

[8]*Quantum Technology Institute, Korea Research Institute of Standards and Science (KRISS), Daejeon 34113, Korea*

[9]*Center for Artificial Low Dimensional Electronic Systems, Institute for Basic Science (IBS), Pohang 37673, Republic of Korea*

*† These authors contributed equally to this work.*

*(C. J.) e-mail: cujang@kist.re.kr, Tel: +82-2-958-6713. (J. C.) e-mail: junwoo@kist.re.kr, Tel: +82-2-958-6445. (H. R.) e-mail: hryu@kist.re.kr, +82-2-958-5705.

## Abstract

Identifying material parameters affecting properties of ferromagnets is key to optimize materials better suited for spintronics. Magnetic anisotropy is of particular importance in van der Waals magnets, since it not only influences magnetic and spin transport properties, but also is essential to stabilizing magnetic order in the two dimensional limit. Here, we report that hole doping effectively modulates the magnetic anisotropy of a van der Waals ferromagnet, and explore the physical origin of this effect. $Fe_{3-x}GeTe_2$ nanoflakes show a significant suppression of the magnetic anisotropy with hole doping. Electronic structure measurements and calculations reveal that the chemical potential shift associated with hole doping is responsible for the reduced magnetic anisotropy by decreasing the energy gain from the spin-orbit induced band splitting. Our findings provide an understanding of the intricate connection between electronic structures and magnetic properties in two-dimensional magnets and propose a method to engineer magnetic properties through doping.

## Keywords

*van der Waals ferromagnets, $Fe_3GeTe_2$, magnetic anisotropy, electronic structures, doping effects*

Layered materials composed of two dimensional (2D) planes that are stacked by van der Waals (vdW) interactions have been extensively investigated. vdW materials exhibit interesting electronic, magnetic, and optical properties such as charge density wave, two-dimensional superconductivity, strong excitonic coupling, and valley dependent optical responses.[1-3] In particular, magnetism in the 2D limit is an intriguing subject in which the role of spin-orbit coupling (SOC) providing magnetic anisotropy is crucial for long range magnetic order.[4, 5] The weak inter-layer coupling and flexible lateral configurations of vdW materials, along with the tunability of magnetic properties (magnetic anisotropy and SOC) through external parameters (strain, gating, proximity effect, Moiré potential, and optical excitation), provide model systems for exploring new and diverse phenomena in 2D magnetism. Moreover, heterostructures based on magnetic vdW materials can be utilized in various valleytronics and spintronics device applications.[6, 7]

Various vdW materials showing robust ferromagnetism in the ultrathin limit have been discovered, such as monolayer $CrI_3$,[8, 9] $Cr_2Ge_2Te_6$,[10] $Cr_2Si_2Te_6$,[11] $VSe_2$,[12] $MnSe_2$,[13] and $Fe_3GeTe_2$.[14] $Fe_3GeTe_2$ is a fundamentally interesting material that exhibits large intrinsically driven anomalous Hall effect (AHE).[15] Its high Curie temperature ($T_c$) relative to other 2D ferromagnetic materials, along with its highly tunable magnetic properties by changing the chemical composition, layer thickness, and external gating makes $Fe_3GeTe_2$ a strong candidate for spintronic devices.[16, 17] In particular, voltage dependent change of $T_c$,[17] and composition dependent change of the AHE[15] was observed in $Fe_3GeTe_2$. In those studies, it is shown that simple yet subtle changes in the electronic structure lead to significant modifications to the magnetic properties. The strong dependence of intrinsic magnetic properties (e.g. $T_c$, AHE) on the chemical potential (doping) by compositional change or voltage gating, suggests that a thorough investigation on

doping-dependent electronic structures of $Fe_3GeTe_2$ is required to fully understand its magnetic properties.

In this paper, we report doping dependent magnetic properties and electronic structures of $Fe_{3-x}GeTe_2$. The magnetic properties of thin layers of $Fe_{3-x}GeTe_2$ ($x \sim 0.36$), measured by magneto-optic Kerr effect (MOKE), show a drastic suppression of the magnetic coercivity and perpendicular magnetic anisotropy (PMA) with hole doping. The investigation of doping dependent changes in the electronic structures by angle-resolved photoelectron spectroscopy (ARPES) and first-principles density functional theory (DFT) reveals that the decrease in PMA is due to the reduction of the electron pockets which possess strong spin-orbit induced band splitting that dominantly contributes to the PMA. We will discuss how our findings can be used to interpret earlier reports on controlling magnetic properties of $Fe_3GeTe_2$,[15, 17] thereby providing a unified understanding of the modulation of magnetism with electronic structure changes. Moreover, we emphasize that the magnetic anisotropy is one of the most important material parameters that determines magnetic and spin transport properties (e.g. magnetic domain phase, current induced magnetization switching). There has been great effort in spintronics research for developing an effective scheme for controlling magnetic anisotropy in spin devices, such as the voltage induced magnetic anisotropy reduction for low power magnetization switching.[18, 19] We believe our method (hole and electron doping) to control the magnetic anisotropy provides an important step for the development of efficient 2D ferromagnet based spin devices.

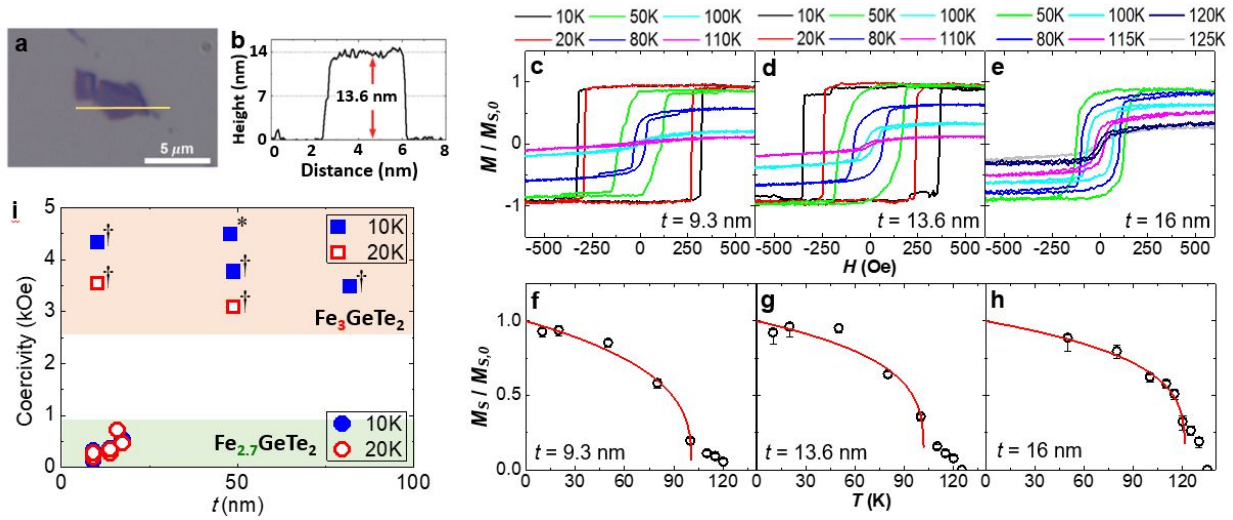


**Figure 1.** **a**, Optical microscope image of a mechanically exfoliated $Fe_{3-x}GeTe_2$ flake on a $SiO_2$/Si substrate. **b**, Height profile measured by AFM along the orange line in **a**. **c-e**, Temperature dependent out-of-plane *M-H* loops of $Fe_{3-x}GeTe_2$ flakes measured by MOKE at several representative thicknesses (*t*). (*M-H* loops for thicker $Fe_{3-x}GeTe_2$ are shown in SI Figure S1) **f-h**, Temperature dependent $M_S$ extracted from **c-e**, and the *M-T* fitting curves (red solid lines). The magnetization in **c-h** is normalized by the extrapolated $M_S$ at $T = 0$ ($M_{S,0}$) obtained from the fitting in **f-h**. **i**, Comparison of the coercivities of Fe deficient $Fe_{3-x}GeTe_2$ and $Fe_3GeTe_2$. The $Fe_3GeTe_2$ data are taken from ref. 20 [square data points marked †][20] and ref. 14 [square data points marked *][14].

The exfoliated $Fe_{3-x}GeTe_2$ (x ~ 0.36) flakes display defect-less flat surfaces (Figure 1a) with the thickness obtained from the height profiles measured by atomic force microscopy (AFM) (Figure 1b). The out-of-plane magnetic hysteresis loops (Figure 1c-e) show square loops with nearly full remanence at low temperatures ($T \leq 80$ K), implying that the thin $Fe_{3-x}GeTe_2$ layers have a uniaxial out-of-plane magnetic easy axis, i.e. they have PMA. The robust PMA is crucial for stabilizing the long-range magnetic order in thin layers of $Fe_{3-x}GeTe_2$.[4, 5] The magnetic coercivity decreases as the temperature increases, typical for magnetic systems approaching the 2D regime. The saturation magnetization ($M_s$) also decreases with increasing temperature (Figure

1f-h), and a ferromagnetic-paramagnetic phase transition is observed at the $T_c$. The $T_c$ of the flakes determined by fitting the *M-T* data (see Supporting Information (SI) for the fitting details) are 101~121 K, slightly increasing with thickness.

In contrast to the moderate change of $T_c$ and coercivity with thickness, we find significant change in both values with Fe content (hole doping). First, the Curie temperature of $Fe_{3-x}GeTe_2$ (~ 100 K for ~ 10 nm layers) is significantly lower than $Fe_3GeTe_2$ (~ 150 K for ~ 10 nm layers).[17, 20] Second, the thin $Fe_{3-x}GeTe_2$ flakes show large reduction in the magnetic coercivity (~ 300 Oe for ~ 10 nm layers, $T$ = 10 K), significantly smaller than $Fe_3GeTe_2$ (~ 4000 Oe for ~ 10 nm layers, $T$ = 10 K)[14, 20] (summarized in Figure 1i). The Fe deficiency in $Fe_3GeTe_2$ provides significant modification to the magnetic transition temperature and coercivity. For the micron sized $Fe_{3-x}GeTe_2$ flakes used in this study, the easy axis coercivity is roughly proportional to the uniaxial magnetic anisotropy (see SI).[21] Therefore, the large reduction in coercivity implies that $Fe_{3-x}GeTe_2$ has significantly smaller, albeit still perpendicular, magnetic anisotropy compared to $Fe_3GeTe_2$. The decrease of Curie temperature and coercivity with Fe deficiency has been reported in *bulk* $Fe_{3-x}GeTe_2$.[22] Also, from earlier reports on the hard-axis (in-plane) hysteresis loops of *bulk* $Fe_3GeTe_2$ and $Fe_{3-x}GeTe_2$,[23-25] we estimate roughly 7 fold decrease in the magnetic anisotropy due to the Fe deficiency. In our study, we find that the decrease in magnetic anisotropy holds true down to the ultrathin regime.

Considering that the magnetic anisotropy is an all-important parameter that stabilizes the magnetic ordering and determines spin transport characteristics, we examine the origin of the Fe content dependent magnetic anisotropy of the $Fe_{3-x}GeTe_2$ using X-ray magnetic circular dichroism (XMCD), ARPES, and DFT calculations (See SI for XMCD results). Since the magnetic

anisotropy decreases with Fe content in both bulk and thin layers, the measurements and calculations in the following sections are conducted with bulk $Fe_{3-x}GeTe_2$.

The relation between the reduced PMA and hole doping is investigated by DFT calculations. We focus on the dependence of the magnetic moments and magnetocrystalline anisotropy energy (MAE) on the hole doping, in which the MAE is defined as the total energy per formula unit (f.u.) with in-plane ([210]) magnetization (IPM) relative to that with out-of-plane ([001]) magnetization (OPM); positive MAE indicates PMA. (We find negligible MAE dependence on the in-plane magnetization directions (see SI) in line with previous DFT results.[26])

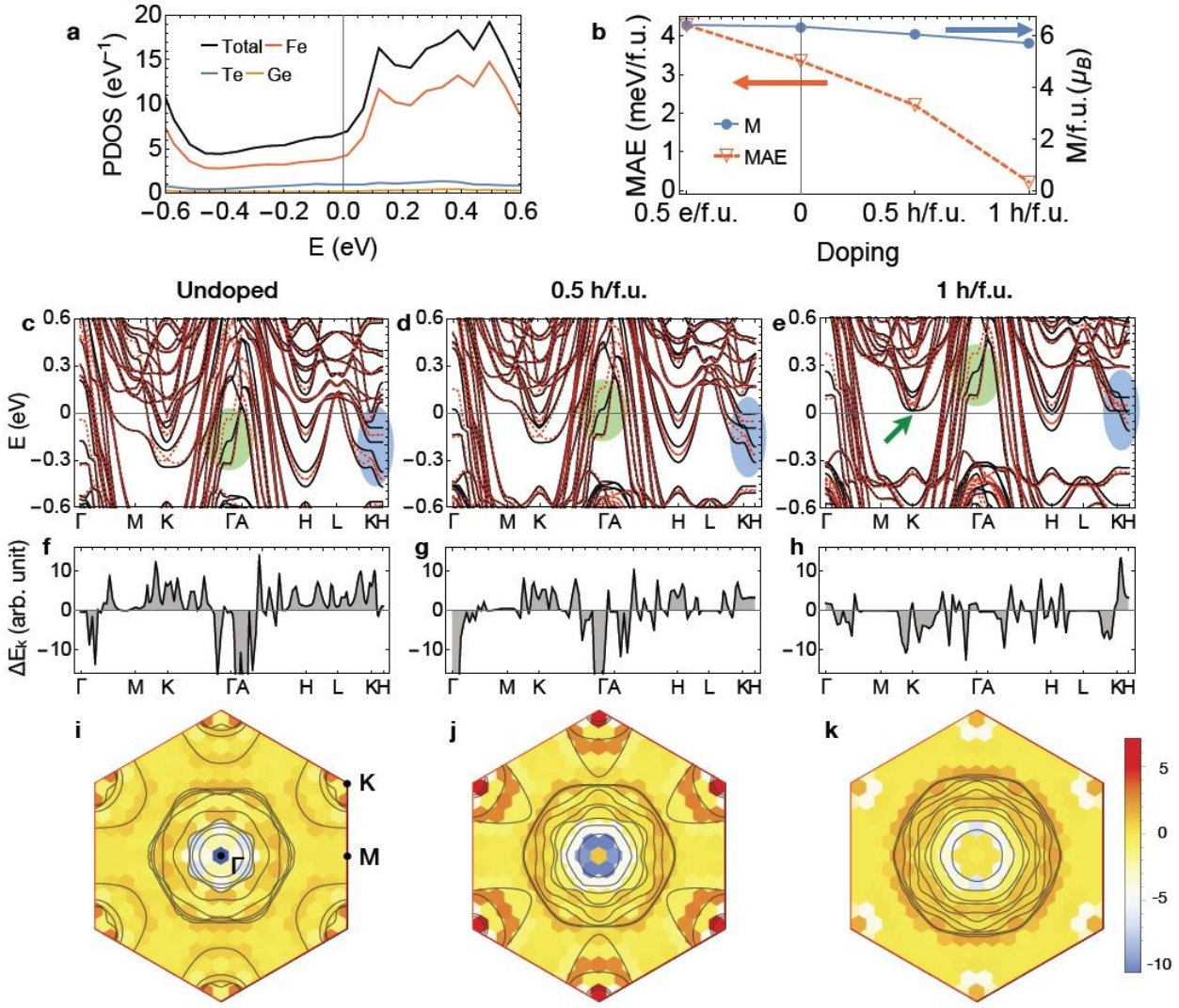

**Figure 2. Calculated electronic band structures and momentum dependent MAE of $Fe_{3-x}GeTe_2$ as a function of hole doping.** **a.** PDOS around the Fermi energy. **b.** MAE and magnetization per f.u. as a function of doping. **c-e**. Band structures with OPM (black solid lines) and IPM (red dotted lines). **d-f**. Momentum-resolved MAE along the high-symmetry lines. **g-i**. Momentum-resolved MAE summed for out-of-plane momentum. The black solid lines are Fermi surfaces with $k_z = 0$. The panels (**c**, **f**, **i**), (**d**, **g**, **j**), and (**e**, **h**, **k**) are for pristine, 0.5 h/f.u., and 1 h/f.u doped $Fe_3GeTe_2$, respectively.

Figure 2a shows the projected density of states (PDOS), which reveals that the majority of the density of states is derived from Fe states responsible for ferromagnetism. Upon hole doping, there is a small reduction in magnetization relative to the pristine $Fe_3GeTe_2$, 5% for 0.5 h/f.u. and 10% for 1 h/f.u., whereas the reduction in MAE is much larger, 33% for 0.5 h/f.u and 93% for 1 h/f.u. (Figure 2b). This strongly suggests that the drastic reduction of MAE is not likely from the decreased spin moments but from the change in SOC. Since the valence of Fe ions in $Fe_{3-x}GeTe_2$ is expected to be in between $Fe^{3+}$ and $Fe^{2+}$,[24, 25] the 1 h/f.u. doping corresponds to a Fe deficiency of x = 0.33 - 0.5, close to x ~ 0.36 of the $Fe_{3-x}GeTe_2$ measured in this study; the ten-fold decrease in MAE is consistent with the large reduction of coercivity and magnetic anisotropy observed by MOKE.

In order to understand the relationship between the MAE and the chemical potential shift associated with the hole doping, we investigate the change in band structure with magnetization directions. We define the momentum dependent MAE as[27, 28]

$$\Delta E_{\boldsymbol{k}} = \frac{1}{N}\sum_{n}\left(f\left(\epsilon_{n\boldsymbol{k}}^{IPM}\right)\epsilon_{n\boldsymbol{k}}^{IPM} - f\left(\epsilon_{n\boldsymbol{k}}^{OPM}\right)\epsilon_{n\boldsymbol{k}}^{OPM}\right) = \frac{1}{N}\sum_{n}\left\{\frac{\epsilon_{n\boldsymbol{k}}^{IPM} + \epsilon_{n\boldsymbol{k}}^{OPM}}{2}\left(f\left(\epsilon_{n\boldsymbol{k}}^{IPM}\right) - f\left(\epsilon_{n\boldsymbol{k}}^{OPM}\right)\right) + O(|\epsilon_{n\boldsymbol{k}}^{IPM} - \epsilon_{n\boldsymbol{k}}^{OPM}|)\right\}, \quad (1)$$

where $\epsilon_{n\boldsymbol{k}}^{IPM}$ and $\epsilon_{n\boldsymbol{k}}^{OPM}$ are eigenvalues with IPM and OPM, respectively, $N$ is the number of $k$-points, and $f(\epsilon)$ is the Fermi-Dirac distribution. The second equation is derived using the eigenvalues at the Fermi energy ($\epsilon_F \sim 9$ eV) much larger than the SOC energy: positive (negative) MAE for $\epsilon_{n\boldsymbol{k}}^{IPM} < \epsilon_F < \epsilon_{n\boldsymbol{k}}^{OPM}$ ($\epsilon_{n\boldsymbol{k}}^{IPM} > \epsilon_F > \epsilon_{n\boldsymbol{k}}^{OPM}$) around the Fermi energy. Figure 2c-e show band structures with IPM and OPM. Around the Γ-A line (green shaded region), we find $\epsilon_{n\boldsymbol{k}}^{IPM} > \epsilon_F > \epsilon_{n\boldsymbol{k}}^{OPM}$, resulting in a negative MAE (Figure 2f-h), whereas around the K-H line (blue shaded region), we find $\epsilon_{n\boldsymbol{k}}^{IPM} < \epsilon_F < \epsilon_{n\boldsymbol{k}}^{OPM}$ from lifted degeneracy with OPM,[15] resulting in a positive MAE (Figure 2f-h).

To investigate the origin of the reduced MAE by hole doping, $\Delta E_{\boldsymbol{k}}$ is summed for the out-of-plane momentum (Figure 2i-k). We first emphasize that the MAE contribution is positive around the K points (electron pockets), and negative around the Γ points (hole pockets). Compared with the pristine $Fe_3GeTe_2$, the doping of 0.5 h/f.u. increases the positive contribution around the K point but also enhances the negative contribution around the Γ point, resulting in an overall reduction of total MAE (Figure 2g, j). The mechanism of hole doping induced MAE reduction is clearly identified when an additional 0.5 h/f.u. is introduced for a total of 1 h/f.u.. In Figure 2h, k we observe the electron pockets around the K point almost vanishing, and also the contribution from the hole pockets is strongly suppressed since the majority of energy shifts along the Γ-A line is shifted above the Fermi energy. Thus, with hole doping, the bands with large spin-orbit induced changes are pushed away from the Fermi energy by the chemical potential shift, thereby decreasing the MAE. We note that the density of states (DOS) at the Fermi energy is 6.5 and 4.1 $eV^{-1}$ for pristine $Fe_3GeTe_2$ and 1 h/f.u. doped $Fe_{3-x}GeTe_2$, respectively, showing only a moderate decrease with hole doping. This indicates that the momentum dependence of the band structures is important in understanding the drastic decrease in MAE (See SI for details). In addition to the hole doped

cases, we find that electron doping of 0.5 e/f.u. increases the MAE by 30% relative to the pristine $Fe_3GeTe_2$ (Figure 2b), due to the increased *k*-space volume of the positive MAE (See SI for the band structures and momentum resolved MAE for the electron doping case).

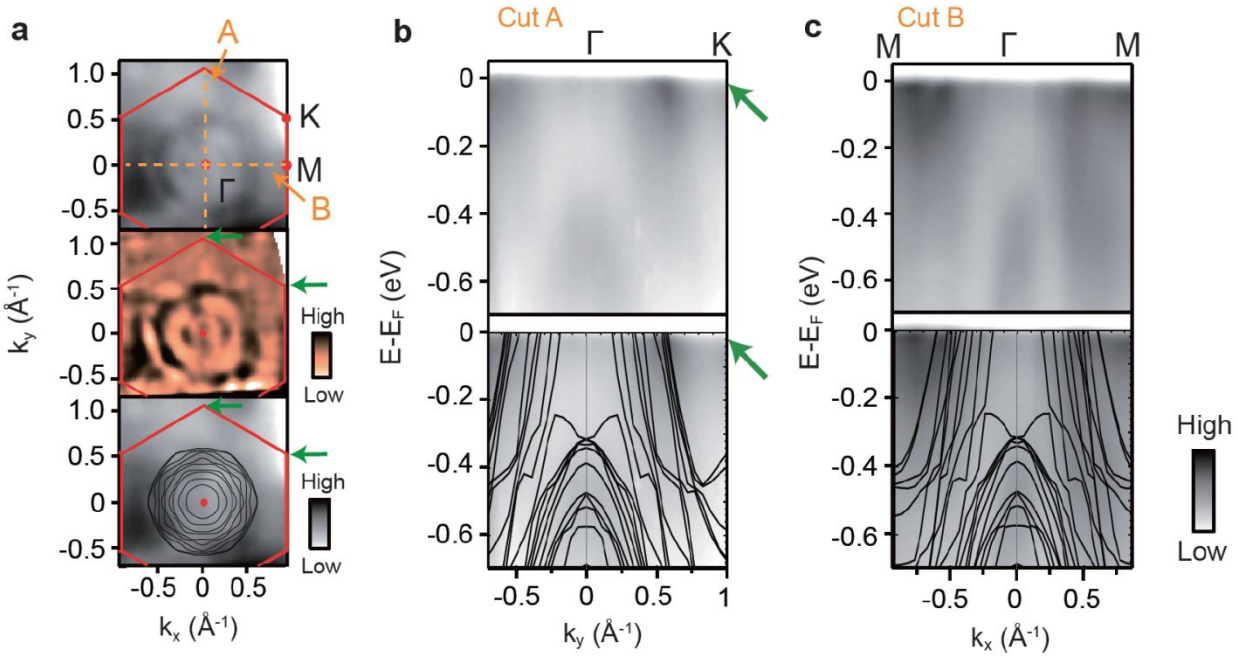


**Figure 3. Electronic band structures of $Fe_{3-x}GeTe_2$ single crystals. a**, Fermi surface measured by ARPES (upper panel), the second-derivative ARPES spectra of the Fermi surface (middle panel), and the calculated Fermi surface for 1 h/f.u. (from Figure 2k) marked by black solid lines overlapped with the ARPES spectra (lower panel). The Brillouin zone is marked by the red solid line. **b**, **c**, Band dispersions along the high symmetry directions (dotted lines A and B in **a**) with the calculated band dispersion (black solid lines) for 1 h/f.u. (from Figure 2e).

In order to confirm the calculated electronic band structures, we performed ARPES measurements on $Fe_{3-x}GeTe_2$ single crystals. Compared to earlier reports on the band structure of pristine $Fe_3GeTe_2$,[15] a Fermi-level shift is observed in that of $Fe_{3-x}GeTe_2$ measured in this study (enlarged hole pockets and disappearance of electron pockets) implying that the Fe deficiency

effectively results in hole doping of $Fe_3GeTe_2$ (See SI for details). The disappearance of the occupied states of the electron pockets around the K point is clearly shown in the Fermi surface (green arrows in Figure 3a) and in the Γ-K cut (green arrows in Figure 3b and 2e) confirming the Fermi energy shift expected from the DFT calculations, and thus supporting the mechanism of chemical potential shift induced MAE reduction.

The mechanism of doping dependent electronic structure modification that we identify can be applied to other interesting phenomena that $Fe_3GeTe_2$ and $Fe_{3-x}GeTe_2$ exhibit. One such observable is the large AHE,[15] induced by the Berry phase from the lifting of the band degeneracy along the K-H lines around the electron pockets.[15] A large AHE is expected when the Fermi energy crosses the electron pockets, consistent with the reported AHE for both pristine and hole doped $Fe_3GeTe_2$;[25] the decreased AHE of hole doped $Fe_3GeTe_2$[15, 25] can be qualitatively understood by the reduced surface area of the electron pockets with hole doping. Our mechanism is also consistent with the voltage induced enhancement of the $T_c$ in ultrathin $Fe_3GeTe_2$,[17] in which the increased surface area of electron pockets by *electron* doping could play an important role. The *increase* of MAE with *electron* doping could be responsible for the increase of the $T_c$, considering that $T_c$ fundamentally increases with magnetic anisotropy.[4] In fact, our DFT calculation shows 30% increase in MAE with doping of 0.5 electron/f.u. (Figure 2b). Thus, according to our mechanism of doping induced band structure change, we believe that there are positive correlations between the coercivity, MAE, AHE, and $T_c$, thereby providing a unifying scheme for understanding the modulation of magnetic properties of a vdW ferromagnet $Fe_3GeTe_2$. Moreover, we believe the doping effect on the magnetic properties of vdW ferromagnets, that we experimentally observe in this study, can be potentially utilized in 2D material based spintronic devices by providing an effective way to manipulate the magnetic anisotropy of 2D vdW ferromagnets.

In conclusion, a large hole doping induced magnetic anisotropy reduction is observed in $Fe_{3-x}GeTe_2$. DFT calculations show that the sharp decrease in MAE is due to changes in the electronic structure, in which the majority of bands that are strongly affected by spin-orbit coupling are shifted away from the Fermi energy by hole doping, thereby reducing the energy gain by spin-orbit induced change in the band structures. The electronic structures of $Fe_{3-x}GeTe_2$ measured by ARPES show significant chemical potential shifts with enlarged hole and reduced electron pockets, supporting the mechanism of electronic structure driven change in the magnetic anisotropy.

## Experimental Section

**Single crystal growth.** Single crystals of $Fe_{3-x}GeTe_2$ were grown from molten metallic fluxes as described previously.[24]

**Magnetic characterization of $Fe_{3-x}GeTe_2$.** Low temperature magnetic hysteresis loops of the exfoliated $Fe_{3-x}GeTe_2$ flakes were measured using a polar (out-of-plane) MOKE system. The MOKE system uses a 408 nm diode laser with a laser spot size ~ 2 micron, and has Kerr rotation detection sensitivity < 0.1 mrad. The XMCD spectroscopy measurements on $Fe_{3-x}GeTe_2$ and $Fe_3GeTe_2$ (*in-situ* cleaved bulk single crystals) were done at Pohang Light Source beamline 2A.

**ARPES measurement.** ARPES measurements were performed at the HERS endstation of the Beamline 10.0.1, Advanced Light Source, Lawrence Berkeley National Laboratory. The ARPES system is equipped with a Scienta R4000 electron analyzer and has base pressure $3\times10^{-11}$ Torr. The photon energy was set at 55 eV with energy and angular resolution of 25 meV and 0.1 degree. Measurements were made at the temperature 15 K.

**First-principles calculations.** We perform first-principles density-functional-theory calculations using the Vienna ab-initio simulation package.[29, 30] The Perdew-Becke-Erzenhof parametrization[31]

for the exchange-correlation functional is used with the projector augmented wave method.[32] The energy cutoff of 600 eV, k-point sampling on a Γ-centered 16×16×5 grid, and the experimental atomic structure were used. The MAE is determined by the force theorem.[27, 28] We confirm that the calculated energy differences relative to self-consistent calculations are within 3%. Simulation with hole doping is treated by reducing the total number of electrons with compensating uniform background charge.

## Supporting Information

Magnetic properties of $Fe_{3-x}GeTe_2$ flakes, Correlation between coercivity and magnetic anisotropy and magnetic domains, Fe spin and orbital moments of $Fe_{3-x}GeTe_2$ and $Fe_3GeTe_2$ determined by XMCD spectroscopy, MAE by force theorem compared with MAE by self-consistent calculations, Dependence of MAE on the in-plane magnetization angles, Band structures and momentum dependent MAE for electron doped $Fe_3GeTe_2$, Density of states of $Fe_{3-x}GeTe_2$ as a function of doping, Electronic band structures of $Fe_{3-x}GeTe_2$ flakes

## Acknowledgements

This work was mainly supported by the KIST Institutional Program (2E29410), the Institute for Basic Science in Korea (Grant No. IBS-R009-D1), and the National Research Council of Science and Technology (NST) grant by MSIP (Grant No. CAP-16-01-KIST). This paper was also supported by the US DOE-BES, Division of Materials Science and Engineering, under Contract No. DESC0012704 (BNL). J. W. C. and H. R. acknowledge the travel fund supported by the National Research Foundation of Korea (NRF) funded by the the Korea government (MSIT) (2019K1A3A7A09033388). The ARPES performed at the ALS was supported by the Office of

Basic Energy Sciences, US DOE, under contract No. DE-AC02-05CH11231. C. H. also acknowledges support from the National Research Foundation of Korea (NRF) grant funded by the Korea government (MSIT) (No. 2017K1A3A7A09016384 and No. 2018R1A2B6004538).

## Conflict of Interest

The authors declare no conflict of interest.

## References

(1) Joe, Y. I.; Chen, X. M.; Ghaemi, P.; Finkelstein, K. D.; de la Pena, G. A.; Gan, Y.; Lee, J. C. T.; Yuan, S.; Geck, J.; MacDougall, G. J.; Chiang, T. C.; Cooper, S. L.; Fradkin, E.; Abbamonte, P. Emergence of charge density wave domain walls above the superconducting dome in 1*T*-$TiSe_2$. *Nature Phys.* **2014,** 10 (6), 421-425.

(2) Cao, Y.; Fatemi, V.; Fang, S.; Watanabe, K.; Taniguchi, T.; Kaxiras, E.; Jarillo-Herrero, P. Unconventional superconductivity in magic-angle graphene superlattices. *Nature* **2018,** 556 (7699), 43.

(3) Wilson, J. A.; Di Salvo, F.; Mahajan, S. Charge-density waves and superlattices in the metallic layered transition metal dichalcogenides. *Advances in Physics* **1975,** 24 (2), 117-201.

(4) Bander, M.; Mills, D. L. Ferromagnetism of ultrathin films. *Phys. Rev. B* **1988,** 38 (16), 12015-12018.

(5) Mermin, N. D.; Wagner, H. Absence of Ferromagnetism or Antiferromagnetism in One- or Two-Dimensional Isotropic Heisenberg Models. *Phys. Rev. Lett.* **1966,** 17 (22), 1133-1136.

(6) Zhong, D.; Seyler, K. L.; Linpeng, X. Y.; Cheng, R.; Sivadas, N.; Huang, B.; Schmidgall, E.; Taniguchi, T.; Watanabe, K.; McGuire, M. A.; Yao, W.; Xiao, D.; Fu, K. M. C.; Xu, X. D. Van der Waals engineering of ferromagnetic semiconductor heterostructures for spin and valleytronics. *Sci. Adv.* **2017,** 3 (5), e1603113.

(7) Samarth, N. Magnetism in flatland. *Nature* **2017,** 546 (7657), 216-218.

(8) Huang, B.; Clark, G.; Navarro-Moratalla, E.; Klein, D. R.; Cheng, R.; Seyler, K. L.; Zhong, D.; Schmidgall, E.; McGuire, M. A.; Cobden, D. H.; Yao, W.; Xiao, D.; Jarillo-Herrero, P.; Xu, X. D. Layer-dependent ferromagnetism in a van der Waals crystal down to the monolayer limit. *Nature* **2017,** 546 (7657), 270.

(9) Thiel, L.; Wang, Z.; Tschudin, M. A.; Rohner, D.; Gutiérrez-Lezama, I.; Ubrig, N.; Gibertini, M.; Giannini, E.; Morpurgo, A. F.; Maletinsky, P. Probing magnetism in 2D materials at the nanoscale with single-spin microscopy. *Science* **2019,** 364 (6444), 973.

(10) Gong, C.; Li, L.; Li, Z. L.; Ji, H. W.; Stern, A.; Xia, Y.; Cao, T.; Bao, W.; Wang, C. Z.; Wang, Y. A.; Qiu, Z. Q.; Cava, R. J.; Louie, S. G.; Xia, J.; Zhang, X. Discovery of intrinsic ferromagnetism in two-dimensional van der Waals crystals. *Nature* **2017,** 546 (7657), 265.

(11) Lin, M. W.; Zhuang, H. L. L.; Yan, J. Q.; Ward, T. Z.; Puretzky, A. A.; Rouleau, C. M.; Gai, Z.; Liang, L. B.; Meunier, V.; Sumpter, B. G.; Ganesh, P.; Kent, P. R. C.; Geohegan, D. B.; Mandrus, D. G.; Xiao, K. Ultrathin nanosheets of $CrSiTe_3$: a semiconducting two-dimensional ferromagnetic material. *J. Mater. Chem. C* **2016,** 4 (2), 315-322.

(12) Bonilla, M.; Kolekar, S.; Ma, Y. J.; Diaz, H. C.; Kalappattil, V.; Das, R.; Eggers, T.; Gutierrez, H. R.; Phan, M. H.; Batzill, M. Strong room-temperature ferromagnetism in $VSe_2$ monolayers on van der Waals substrates. *Nature Nanotech.* **2018,** 13 (4), 289.

(13) O'Hara, D. J.; Zhu, T. C.; Trout, A. H.; Ahmed, A. S.; Luo, Y. K.; Lee, C. H.; Brenner, M. R.; Rajan, S.; Gupta, J. A.; McComb, D. W.; Kawakami, R. K. Room Temperature Intrinsic Ferromagnetism in Epitaxial Manganese Selenide Films in the Monolayer Limit. *Nano Lett.* **2018,** 18 (5), 3125-3131.

(14) Fei, Z. Y.; Huang, B.; Malinowski, P.; Wang, W. B.; Song, T. C.; Sanchez, J.; Yao, W.; Xiao, D.; Zhu, X. Y.; May, A. F.; Wu, W. D.; Cobden, D. H.; Chu, J. H.; Xu, X. D. Two-dimensional itinerant ferromagnetism in atomically thin $Fe_3GeTe_2$. *Nature Mater.* **2018,** 17 (9), 778.

(15) Kim, K.; Seo, J.; Lee, E.; Ko, K. T.; Kim, B. S.; Jang, B. G.; Ok, J. M.; Lee, J.; Jo, Y. J.; Kang, W.; Shim, J. H.; Kim, C.; Yeom, H. W.; Il Min, B.; Yang, B. J.; Kim, J. S. Large anomalous Hall current

induced by topological nodal lines in a ferromagnetic van der Waals semimetal. *Nature Mater.* **2018,** 17 (9), 794.

(16) Drachuck, G.; Salman, Z.; Masters, M. W.; Taufour, V.; Lamichhane, T. N.; Lin, Q. S.; Straszheim, W. E.; Bud'Ko, S. L.; Canfield, P. C. Effect of nickel substitution on magnetism in the layered van der Waals ferromagnet $Fe_3GeTe_2$. *Phys. Rev. B* **2018,** 98 (14), 144434.

(17) Deng, Y. J.; Yu, Y. J.; Song, Y. C.; Zhang, J. Z.; Wang, N. Z.; Sun, Z. Y.; Yi, Y. F.; Wu, Y. Z.; Wu, S. W.; Zhu, J. Y.; Wang, J.; Chen, X. H.; Zhang, Y. B. Gate-tunable room-temperature ferromagnetism in two-dimensional $Fe_3GeTe_2$. *Nature* **2018,** 563 (7729), 94.

(18) Shiota, Y.; Nozaki, T.; Bonell, F.; Murakami, S.; Shinjo, T.; Suzuki, Y. Induction of coherent magnetization switching in a few atomic layers of FeCo using voltage pulses. *Nature Mater.* **2012,** 11 (1), 39-43.

(19) Maruyama, T.; Shiota, Y.; Nozaki, T.; Ohta, K.; Toda, N.; Mizuguchi, M.; Tulapurkar, A. A.; Shinjo, T.; Shiraishi, M.; Mizukami, S.; Ando, Y.; Suzuki, Y. Large voltage-induced magnetic anisotropy change in a few atomic layers of iron. *Nature Nanotech.* **2009,** 4, 158.

(20) Tan, C.; Lee, J.; Jung, S. G.; Park, T.; Albarakati, S.; Partridge, J.; Field, M. R.; McCulloch, D. G.; Wang, L.; Lee, C. Hard magnetic properties in nanoflake van der Waals $Fe_3GeTe_2$. *Nature Commun.* **2018,** 9, 1554.

(21) Cullity, B. D.; Graham, C. D., *Introduction to Magnetic Materials*. 2nd ed.; Wiley Online Library: 2008.

(22) May, A. F.; Calder, S.; Cantoni, C.; Cao, H.; McGuire, M. A. Magnetic structure and phase stability of the van der Waals bonded ferromagnet $Fe_{3-x}GeTe_2$. *Phys. Rev. B* **2016,** 93 (1), 014411.

(23) León-Brito, N.; Bauer, E. D.; Ronning, F.; Thompson, J. D.; Movshovich, R. Magnetic microstructure and magnetic properties of uniaxial itinerant ferromagnet $Fe_3GeTe_2$. *J. Appl. Phys.* **2016,** 120 (8), 083903.

(24) Liu, Y.; Ivanovski, V. N.; Petrovic, C. Critical behavior of the van der Waals bonded ferromagnet $Fe_{3-x}GeTe_2$. *Phys. Rev. B* **2017,** 96 (14), 144429.

(25) Liu, Y.; Stavitski, E.; Attenkofer, K.; Petrovic, C. Anomalous Hall effect in the van der Waals bonded ferromagnet $Fe_{3-x}GeTe_2$. *Phys. Rev. B* **2018,** 97 (16), 165415.

(26) Zhuang, H. L.; Kent, P. R. C.; Hennig, R. G. Strong anisotropy and magnetostriction in the two-dimensional Stoner ferromagnet $Fe_3GeTe_2$. *Phys. Rev. B* **2016,** 93 (13), 134407.

(27) Daalderop, G. H. O.; Kelly, P. J.; Schuurmans, M. F. H. First-principles calculation of the magnetocrystalline anisotropy energy of iron, cobalt, and nickel. *Phys. Rev. B* **1990,** 41 (17), 11919-11937.

(28) Wang, X.; Wang, D.-s.; Wu, R.; Freeman, A. J. Validity of the force theorem for magnetocrystalline anisotropy. *J. Magn. Magn. Mater.* **1996,** 159 (3), 337-341.

(29) Kresse, G.; Joubert, D. From ultrasoft pseudopotentials to the projector augmented-wave method. *Phys. Rev. B* **1999,** 59 (3), 1758-1775.

(30) Kresse, G.; Furthmüller, J. Efficient iterative schemes for ab initio total-energy calculations using a plane-wave basis set. *Phys. Rev. B* **1996,** 54 (16), 11169-11186.

(31) Perdew, J. P.; Burke, K.; Ernzerhof, M. Generalized gradient approximation made simple. *Phys. Rev. Lett.* **1996,** 77 (18), 3865-3868.

(32) Blöchl, P. E. Projector augmented-wave method. *Phys. Rev. B* **1994,** 50 (24), 17953-17979.

# Table of Contents Graphic